



# Geometric design of axial piston machine slipper-bearings made of high-performance plastics

Felix Schlegel<sup>1</sup> · Katharina Schmitz<sup>1</sup>

Received: 13 September 2024 / Accepted: 12 February 2025  
© The Author(s) 2025

## Abstract

Oil hydraulic drivetrains are crucial in several industrial applications due to their high power density and dynamics, making them irreplaceable by electric drives. These systems consist of pumps that convert mechanical power into hydraulic power through pressure and volume flow, with axial piston machines being the most commonly used type. The performance and longevity of these pumps are largely determined by their tribological contacts, particularly the slipper-swashplate contact, which typically consists of a hard-soft material pairing of non-ferrous metal and hardened steel. Copper alloys are usually used, which are often alloyed with 0.1 to 23 % lead to improve malleability, corrosion resistance and emergency running properties. However, lead toxicity and copper's role in accelerating oil aging raise environmental and cost concerns. This study explores the potential of replacing conventional brass slippers with tribologically optimized high-performance plastics. With an FEM-based geometry study several slipper design features are analyzed and their potential for wear reduction are discussed. The focus is on the design of the slipper socket and the attachment of a plastic running surface as well as its influence on the deformation of the running surface. In this context, both conventional non-ferrous metal and plastic slippers are investigated.

## Geometrische Konstruktion von Hochleistungskunststoff-Gleitschuhen für Axialkolbenmaschinen

### Zusammenfassung

Ölhydraulische Antriebsstränge sind aufgrund ihrer hohen Leistungsdichte und Dynamik in zahlreichen industriellen Anwendungen von entscheidender Bedeutung und werden in naher Zukunft durch elektrische Antriebe nicht zu ersetzen sein. In diesen Systemen wandeln Pumpen mechanische Leistung durch Druck und Volumenstrom in hydraulische Leistung. Der am häufigsten genutzte Pumpentyp ist dabei die Axialkolbenmaschine. Die Leistung und Langlebigkeit dieser Pumpen wird weitgehend durch ihre tribologischen Kontakte bestimmt, insbesondere durch den Kontakt zwischen Gleitschuh und Schrägscheibe, der in der Regel aus einer Hart-Weich-Materialpaarung aus Buntmetall und gehärtetem Stahl besteht. Üblicherweise kommen dabei Kupferlegierungen zum Einsatz, die oft mit 0,1 bis 23 % Blei legiert werden, um die Formbarkeit, Korrosionsbeständigkeit und die Notlaufeigenschaften zu verbessern. Die Toxizität von Blei und die Rolle von Kupfer bei der Beschleunigung der Ölalterung werfen jedoch Umwelt- und Kostenprobleme auf. In dieser Studie wird diskutiert, ob tribologisch optimierte Hochleistungskunststoffe ein Ersatz für Buntmetall im Gleitschuh-schrägscheibe Kontakt sein könnten. Anhand einer FEM-basierten Geometriestudie werden verschiedene Designmerkmale von Gleitschuhen analysiert und deren Potenzial zur Verschleißreduzierung diskutiert. Der Fokus liegt dabei auf der Gestaltung des Gleitschuhsockels und der Anbringung einer Kunststoffauflagefläche sowie deren Einfluss auf die Verformung der Lauffläche. In diesem Zusammenhang werden sowohl konventionelle Buntmetall- als auch Kunststoffgleitschuhe untersucht.

✉ Felix Schlegel  
[Felix.Schlegel@ifas.rwth-aachen.de](mailto:Felix.Schlegel@ifas.rwth-aachen.de)

Katharina Schmitz  
[Katharina.Schmits@ifas.rwth-aachen.de](mailto:Katharina.Schmits@ifas.rwth-aachen.de)

<sup>1</sup> Institute for fluid power drives and systems RWTH Aachen,  
Campus Boulevard 30, 52074 Aachen, Germany

# 1 Introduction

Hydraulic drive systems are widely used in technical applications like aviation, industry, mobile machinery and robotics to meet demands for power density, damping, and dynamics [1]. These systems convert mechanical energy into hydraulic energy for efficient power transmission, movement conversion, and generation of comparatively high forces or torques. Typically, an electric motor or combustion engine powers a pump, converting mechanical energy into hydraulic energy, which is then reconverted into mechanical power via a hydraulic motor or cylinder. The type of hydraulic machine most used in industry and research is the axial piston machine (AKM), which can be used both as a pump and as a motor [2]. The tribological contacts of such a machine are usually made from hard-soft material pairings consisting of hardened steel and non-ferrous metals. Due to environmental concerns, including toxic alloy additives and oil aging, alternative materials such as high-performance plastics are being explored, despite challenges in their wear properties. In this context, this paper uses a FEM study to investigate how the geometric design of the slipper-swashplate bearing affects its deformation. As this deformation determines the lubrication gap shape, it directly influences wear due to the gap height-dependent contact pressure distribution. After a comparison of conventional materials with high-performance plastics in Sect. 1.2, design adaptations that may enable the use of polymers are identified. In the second section, the structure of a Finite-Element-Method (FEM) model is introduced, with the help of which various geometric features are analyzed in the third section.

## 1.1 Slipper-bearings in axial piston machines

Axial piston machines use the displacement of a cyclical piston movement to convey a volume flow. A basic distinction is made between three designs: swashplate-, bent-axis- and wobble-plate type machine [1]. The focus of this publication is on the swashplate type, whose functionality is discussed based on its structure shown in Fig. 1 afterwards.

In pump operation, the drive shaft rotates a cylinder block containing multiple pistons. Due to this motion, an angled swash plate forces the pistons into an oscillating movement. A valve plate regulates fluid flow. During the suction stroke, the valve plate connects the piston chambers to the suction line (low pressure LP), causing the extending pistons to draw in fluid. In the delivery stroke, the chambers are connected to the delivery line (high pressure HP), and the retracting pistons push out fluid. High axial forces on the pistons caused by inertia and pressure, are supported by slippers on the swashplate. These slippers are connected to the pistons by ball joints, to ideally follow the swashplate without macroscopic tilting. Nevertheless, those ball joints enable a multi-axis microscopic tilting of the slippers, which enables the formation of a convergent lubrication gap and thus the build-up of a hydrodynamic force. In motor operation the machine works the other way round: pressurized oil pushes the pistons, driving the shaft. The pump's lifetime and efficiency are determined by three key tribological contacts: the slipper-swashplate, the cylinder block-valve plate, and the piston-bushing contact. This paper focuses on the slipper-swashplate contact, which itself consists of three tribological interfaces, that are highlighted in Fig. 1: 1<sup>st</sup> the running surface-swashplate, 2<sup>nd</sup> the slipper-retainer and 3<sup>rd</sup>

**Fig. 1** Structure of an axial piston machine

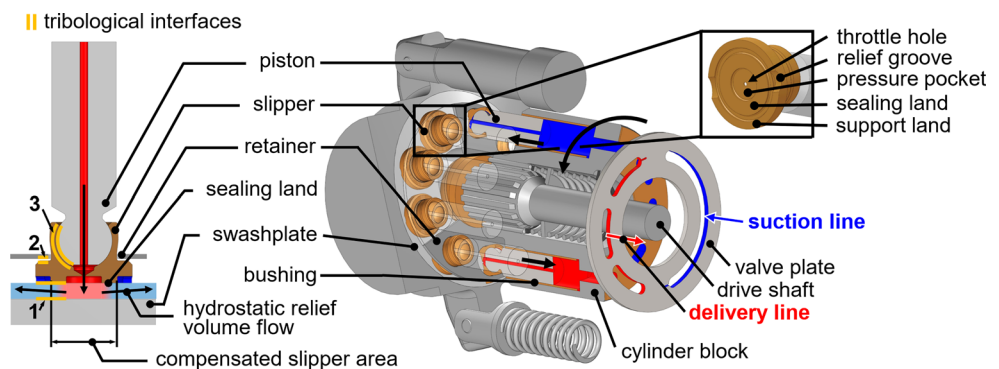
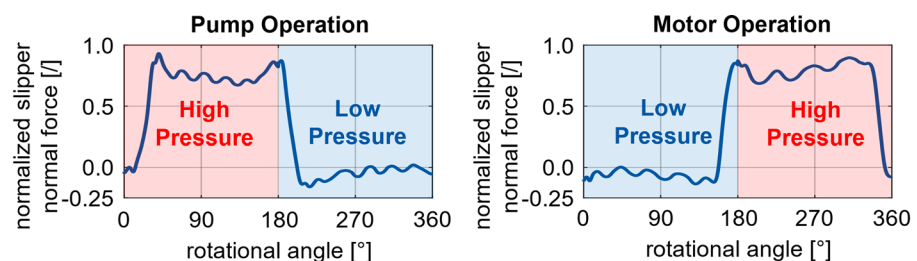


**Fig. 2** Normal force of the slipper-bearing for one pump rotation



the ball joint contact. The running surface-swashplate and the ball joint contact are hydrostatically relieved due to the high normal loads, illustrated in Fig. 1 on the left. A defined leakage flow is diverted from the machine's volume flow and is fed in the tribological contacts via a throttle, reducing the remaining normal load. The design of the so-called compensated slipper area, which forms the sealing gap, allows for setting a defined relief force. The degree of load reduction is referred to as the degree of hydrostatic relief which is usually 92–105 % for the running surface-swashplate [2, 3] and approx. 50 % for the ball joint contact [3]. The course of the remaining normal force is shown in Fig. 2 based on the author's calculations from [4]. Here, a positive force points from the slipper to the swashplate. A detailed analytical description of this force and a study on the influence of operating conditions and pump design parameters can also be found in [4].

As shown in Fig. 2, the load on the slipper alternates between a high and a low-pressure level every 180° of rotation, creating a cyclic load with a frequency twice the machine speed, which can lead to fatigue damage. The highest tribological load occurs during the high-pressure phase at the reversal points. Hydrodynamics and hydrostatic relief can reduce this force, but excessive reduction may cause the normal force on the slipper to become negative, lifting it off the swash plate. On the one hand, this leads to a loss of the sealing function, increasing leakage and on the other hand, macroscopic slipper tilting can occur, causing severe wear. To prevent this, axial piston machines usually contain a retainer, either limiting lift-off height (fixed clearance retainer) or applying additional force that increases with stroke (positive force retainer) [2]. During lift-off the ball joint is exposed to tensile stress due to the retainer's counterforce. This can cause ball cup breakage or expansion, leading to axial play, that enables an impacting load in the joint, potentially causing fatigue-induced failure [5]. Below, fatigue is not considered further, as the mapping of cyclic loads would require a dynamic EHL simulation and fatigue occurs mainly in the joint and not on the running surface, which is the focus of the analysis.

## 1.2 Materials for slipper-bearings

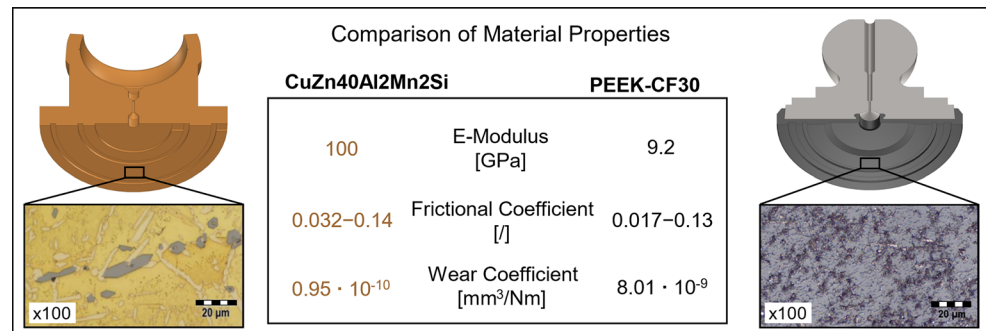
The slipper-swashplate contact is typically made of self-adjusting hard-soft material combinations, such as non-ferrous metals and hardened steel, to enable run-in, the storage of hard particles and the reduction of adhesion risk due to differing lattice structures. Common materials are usually copper-based alloys like brass, bronze, and gunmetal, often alloyed with lead to improve formability, machinability, corrosion resistance, and emergency self-lubrication [6]. A typical conventional lead containing copper alloy for slippers is CuZn40Al2Mn2Si with the brand name Aeterna

3838. However, due to lead's toxicity and copper's tendency to oxidize and catalyze oil degradation, research is focusing on alternatives. There are several approaches for meeting those disadvantages. Holzer et al. [7] and Ivantysyn [8] explored the characteristics of lead-free copper alloys like CuZn36Mn3AlSi1Sn and CuZn28Al4Ni3Si1Mn although this does not eliminate the downsides of copper. Wu [9] examined steel slippers made of 38CrMoAlA and 1Cr18Ni9Ti, that showed higher frictional coefficients than typical non-ferrous metal alloys and have a significant adhesion risk. Kalin et al. [10] investigated Diamond-Like-Carbon (DLC) coatings and Schuhler [11] tested DLC-WC (tungsten carbide) coatings. Similar tests were also carried out by Rizzo for nanocoated [12] and by Tang [13] for MoS<sub>2</sub> coated slippers. Basically, those coatings can prevent adhesion and lower friction, but due to thin layer thickness and scratch sensitivity, the contact is no longer self-adjusting, which limits lifetime. Holzer et al. [14] investigated metal matrix composite coatings like 316L(75 vol.%) and SiC (25 vol.%) in axial piston machines, that provide a greater layer thickness, but which lead to hard wear particles in the hydraulic system. There are more approaches for new slipper materials, however, a particularly promising approach, which is considered below, is the use of polymers, as they combine the advantages of a hard-soft pairing with particularly low frictional coefficients, whereby increased deformation and wear represent hurdles.

## 1.3 Plastic slippers and research objective

The use of plastics in oil-hydraulic applications has been little researched to date. With a general analysis, Stryczek [15] shows that fluid power components made of plastic can be used and that the performance depends on the design of the components. More extensive work exists on the use of plastic in water-hydraulic applications. In this context, plastic slippers for axial piston pumps have been explicitly researched and there is already a commercially available water pump series from Danfoss GmbH that uses plastic slippers (look at [16]). However, the main reason for the use of plastic slippers in water hydraulics is not the avoidance of lead and copper, but the poorer lubricating properties of water and the lower friction of plastic. In his review [17], Yang provides a basic overview of various tribological studies on plastic-steel pairings under water lubrication and discusses their use in axial piston pumps. Therefore, only studies that explicitly refer to slippers are discussed below. Liu [18] conducted a material screening of plastic slippers made from fiber-filled phenol, carbon fiber-reinforced (CFR) polyamideimide (PI), and polyetheretherketone (PEEK) against mating surfaces of 1Cr18Ni9Ti, 2Cr13, and ZrO<sub>2</sub>-coated 1Cr18Ni9Ti. Based on wear volume measurements, he concluded that plastic

**Fig. 3** Comparison of slipper materials (reflected light microscope pictures)



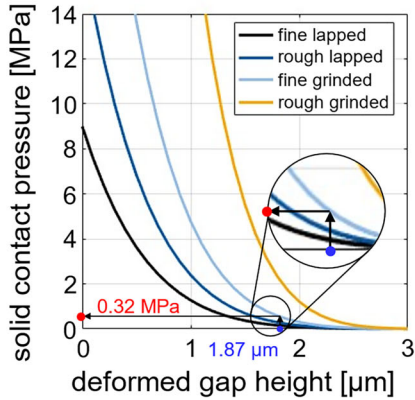
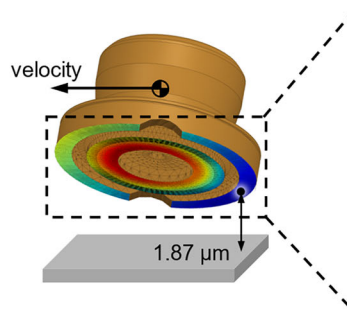
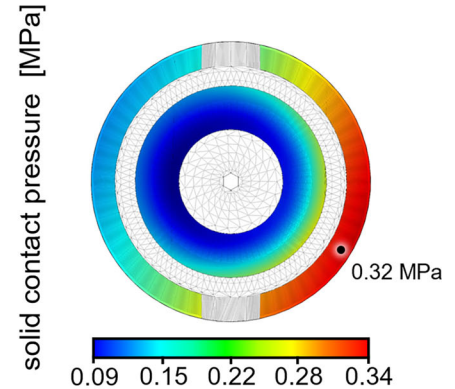
slippers are suitable for common water pumps. However, due to the lack of geometric data for the test specimens, the wear volumes cannot be converted into standard wear coefficients, such as those from Archard's law [19]. Ma [20] investigated theoretical and experimentally the influence of the sea depth on the leakage mechanisms of polymer slippers in seawater AKM. Li [21] compared experiments with CFR-PEEK against 316L and 1Cr17Ni2 steel under water lubrication using a “pin-on-disc” tribometer and real plastic slippers in a water AKM. He observed greater steel wear in the AKM, with no significant change in the plastic. The measured wear coefficients were on the order of  $10^{-7}$  mm<sup>3</sup>/Nm. Li found that hydrostatic pressure affects wear, attributing it to the micro deformation of the polymer matrix causing the graphite fibers to bear more load. Guan [22] previously demonstrated this effect using a disc-on-disc tribometer with CFR-PEEK and 431SS in water lubrication. Furthermore, Li investigated the failure mechanisms of the ball-joint contact of plastic slippers in [23] and he carried out a calculation study on the heat input into water during operation of a water AKM in [24]. Nie investigates in [25] the performance and wear of a water hydraulic plastic slipper depending on an annular orifice damper. He calculates the slipper's normal force and performs a sensitivity analysis of the load carrying capacity depending on the design of the damper. Rokala studied the deformation behavior of plastic slippers experimentally and through simulations [26]. He demonstrated that plastic slippers are viable for water-hydraulic applications and that PEEK's pv-limit can be exceeded at higher speeds due to hydrodynamics [27]. However, he noted that increased plastic wear necessitates maximizing the degree of hydrostatic relief. His EHL simulations revealed significant deviations in deformation behavior from conventional slipper design equations, a finding supported by Schoemacker's simulations [28]. Rokala identified a precise understanding of deformation behavior as crucial for optimizing the degree of hydrostatic relief and enabling plastic slipper use. However, his research was limited to a simple one-land slipper without support lands or other common modern design features.

While insights from water pump studies are valuable, this publication focuses on plastic slippers for oil-hydraulic axial piston machines, which operate under different force and lubrication conditions. In [4], the author measured the friction and wear properties of various plastics under typical oil-hydraulic conditions (oil-lubrication in HLP46, 40 °C, relative velocity up to 15 m/s, contact pressure up to 3 MPa) using an abstracted “slipper-on-disc” tribometer. Key material parameters of this study for 30 vol.% CFR-PEEK are shown in Fig. 3.

In [4], the author reaches a similar conclusion as Rokala for water-hydraulic applications. PEEK's dry pv-limit is significantly exceeded under oil lubrication. However, increased wear compared to conventional non-ferrous metals is a challenge and necessitates geometric modifications. The higher elastic modulus and swelling complicate the slipper design. Furthermore, the author conducted an analytical geometry study [29], identifying forces such as mass-, centrifugal-, and hydrodynamic forces as key disturbing factors, whose exact knowledge is necessary for optimizing the degree of hydrostatic relief, alongside the effect of surface deformation discussed by Rokala. Moreover, in [4] the author used a Finite-Element-Method (FEM) geometry study to investigate the influence of various design parameters of the slipper's running surface on its deformation behavior. A load-independent, uniform deformation is not only necessary, to be able to precisely adjust the degree of hydrostatic relief, but also to avoid an uneven contact pattern and thus locally increased solid contact pressure (Fig. 4).

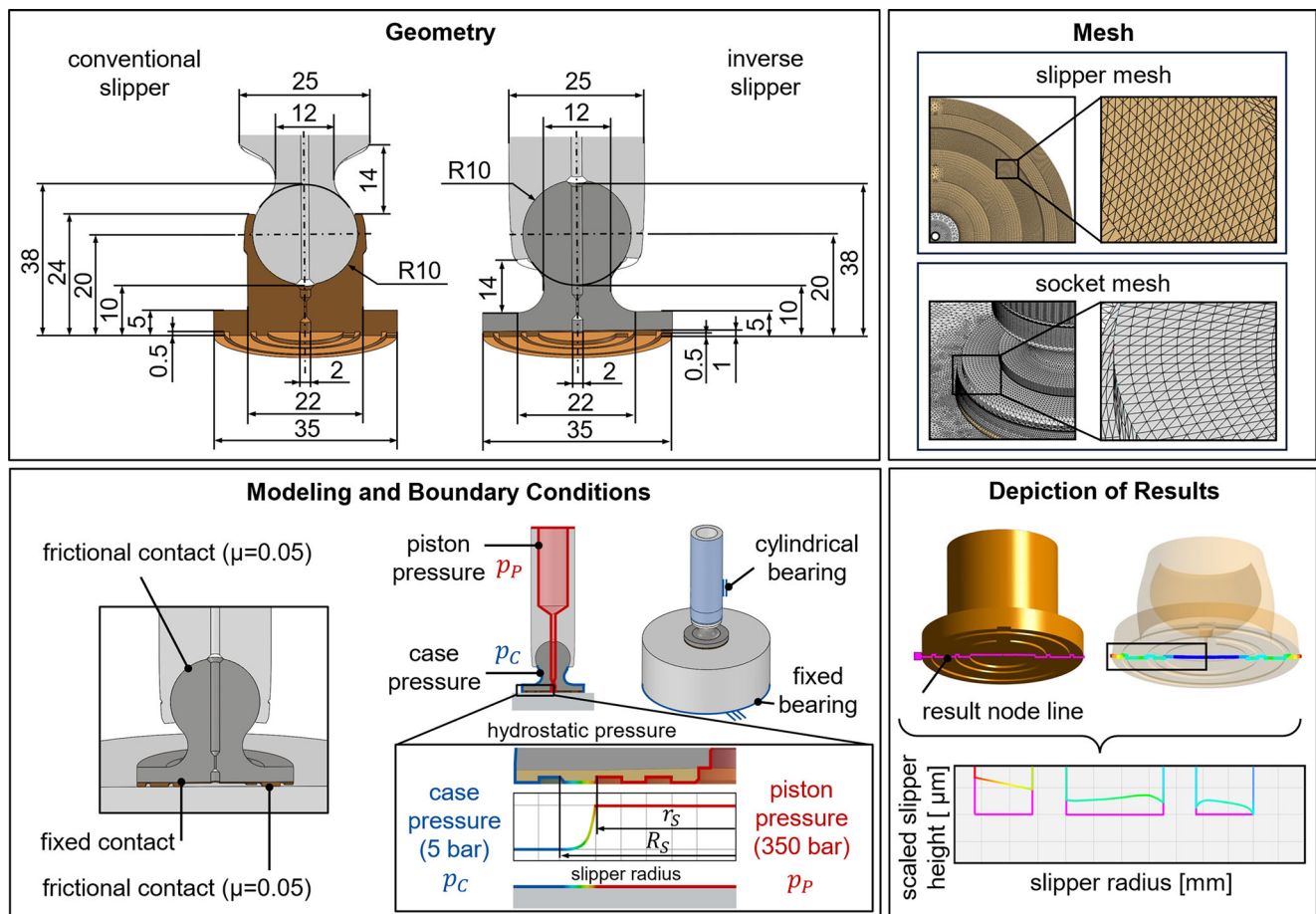
Figure 4 presents an EHL simulation of the contact pattern and solid contact pressure curves for CuZn40Al2Mn2Si in various surface treatment states, calculated using the Greenwood-Williamson and Tripp contact model [30] with MC-Cool's parameter identification [31]. This reveals that even sub-micrometer surface irregularities can cause significant contact pressure variations in the MPa range. For this example, this leads to increased local wear, with the maximum contact pressure being about 1.8 times higher than the nominal pressure, resulting in local wear approximately twice as fast as expected.



**Contact Pressure CuZn40Al2Mn2Si****Slipper Gap****Slipper Contact Pattern****Fig. 4** Typical contact pressure distribution of a slipper-bearing

This paper builds on Rokala's work and the author's prior findings, using an FEM geometry study to explore how the slipper deformation can be controlled. The goal is to prevent wear from localized contact pressure increases and to enable a load-independent optimization of the degree of hydrostatic relief. The study is focusing on the design

of the ball cup socket and the base socket. Initially, the study addresses non-ferrous metal for general applicability. Additionally, it evaluates the fastening mechanism and deformation of plastic slippers.

**Fig. 5** Simulation structure, geometry, boundary conditions and result depiction

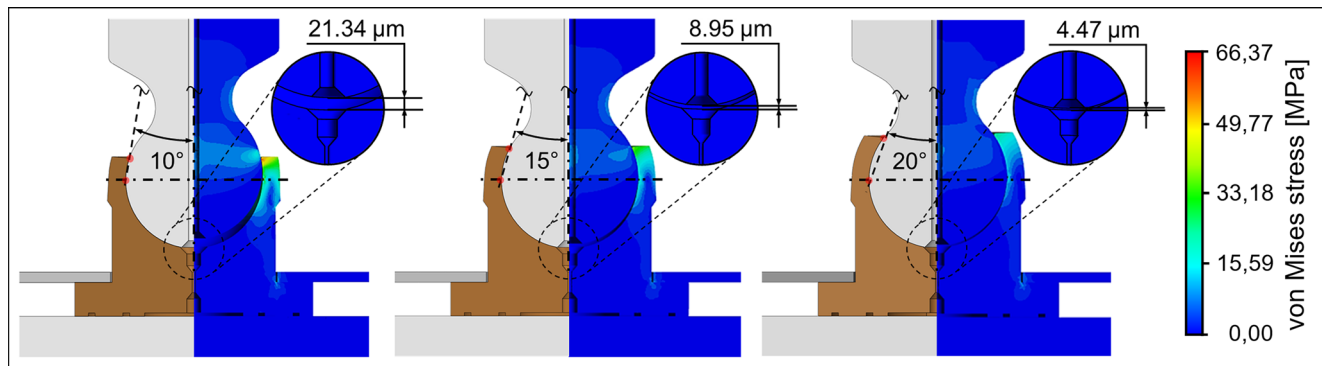


Fig. 6 FEM-Study on axial play and neck tension depending on the wrap angle

## 2 Simulation structure

A structural FEM simulation model based on the software ANSYS Mechanical is used for the geometry study presented in this paper. The direct Ansys MAPDL Solver was used for the solution. The geometry, modeling structure and boundary conditions are shown in Fig. 5. The same basic geometry of the slipper was used for all simulations and only the design feature under discussion was changed.

The simulations account for both piston and swash plate deformations, at a temperature of 40 °C, which is common in oil hydraulics. In this study, the swash plate is modeled as a semi-infinite plate with significantly larger dimensions than the area affected by deformation and is fixed at the underside. All steel parts are modeled as linear 42CrMoV4. The polymer parts are calculated with nonlinear deformation based on stress-strain data from the manufacturer. The applied loads include piston pressure  $p_P$ , case pressure  $p_C$ , and the logarithmic pressure drop of the hydrostatic pressure  $p_{HS}$  calculated from Eq. 1. Where  $r$  is the radial variable,  $r_s$  the sealing lands inner and  $R_s$  the sealing lands outer radius  $R_s$  [2].

$$p_{HS} = p_P \left( 1 - \frac{\ln(r/r_s)}{\ln(R_s/r_s)} \right) \quad (1)$$

Unlike Rokala's simulations, which couple a static FEM with a static flow calculation to account for pressure changes from gap geometry variations, these simulations simplify the process, reducing computation time and complexity. This allows for a broader analysis of geometric features to provide a more general overview. Rokala discusses that this assumption leads to an underestimation of the hydrostatic pressure force, that increases with the piston pressure. For 100 bar piston pressure, Rokala calculated an error of 11.4 % and for 350 bar an error of 22.3 % for his investigated geometry [26]. The results in Sect. 3 are presented along a line with 90° offset from the pressure relief grooves (Fig. 5), facilitating a variant comparison.

## 3 Results and discussion

This chapter presents results on slipper geometry study, focusing on the ball cup, the base socket, and plastic running surface attachments to assess their impact on the slipper's lubrication gap deformation. Typically, the ball cup socket design is determined by the ball joint's geometry and loads rather than surface deformation. As shown in Fig. 2, the ball joint experiences both compressive and tensile stresses, particularly when entering the suction stroke. The stress in the ball cup neck not only depends on its wall thickness and the ball size, but also on the wrap angle, which defines the ball cup overlap area. Figure 6 illustrates that increasing the wrap angle from 10° to 20° under a 600 N tensile load reduces maximum stress from 66.37 MPa to 27.25 MPa and decreases elastic axial play by approx. 17 μm. These stresses would not lead to direct breakage of the slipper due to overload. However, as these stresses are not constant, but oscillates between suction and delivery stroke with each pump revolution, higher stresses will lead to a shorter lifetime due to the materials fatigue strength. It follows from this, that one aim of design should be the reduction of these stresses. Elastic axial play refers to deformation-induced play, that must be distinguished from permanent axial play caused by plastic deformation and wear. Excessive axial play can accelerate fatigue due to the greater impact stroke and possible particle intrusion into the joint can cause severe contact pressure peaks. However, increasing the wrap angle while remaining the piston neck diameter requires a swivel angle (swashplate inclination) reduction due to the slipper tilt limit. To mitigate stress and elastic axial play without reducing the swivel angle, alternative measures like increasing the socket diameter or changing ball size, as shown in Fig. 7, are needed.

Figures 7, 8, 9, 10 and 11 each show the impact of four design features on running surface deformation. The base geometry (Fig. 5) remains unchanged, only the features under investigation, which are displayed below the deformation curves, are varied. As shown in Fig. 5, the

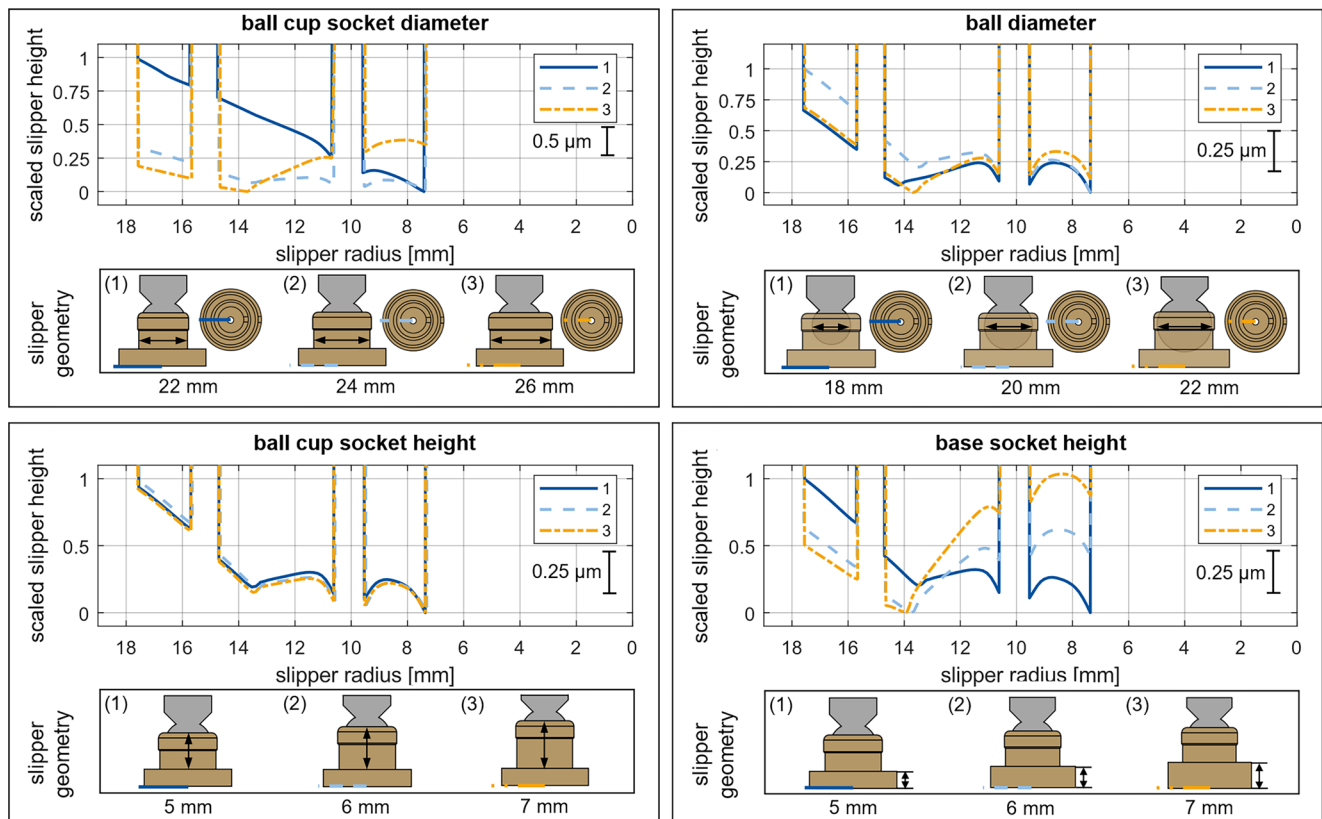


**Fig. 7** Geometry study results for the ball cup socket and ball. Based on the author's prior work, two inner support lands are included in the plastic slipper analysis to reduce overall deformation

results depict the surface deformation along a line, focusing on the left half of the slipper due to symmetry. The curves highlight relative deformation differences caused by changes in individual design features. Figure 7 shows that no clear optimization path exists for the ball cup socket diameter, because lowering its diameter leads to lifting at the inside and increasing its diameter leads to lifting at the outside. A larger diameter reduces stress in the ball cup neck and elastic axial play but lowers the outer running surface and increases deformation due to hydrostatic pressure in the slipper's center. This occurs because the wider ball cup socket transfers the ball force further outward into the base socket, furthermore, affecting where the outer surface bends due to geometrically induced stiffness changes. The ball cup socket height has minimal effect on these phenomena, while ball size shifts the force application point. The base socket height significantly affects deformation, as with increased height more material between the ball and the hydrostatic pressure field can be compressed. Therefore, the ball cup socket diameter and the base socket height must be considered together. The following diagrams depict the same brass slipper with one inner and outer sealing land, with only one feature varied in each case.

Figure 8 depicts that a conical base socket increases running surface deformation, making it undesirable. The defor-

mation effect becomes noticeable only at larger cone angles and seems to be not linear. A conical inner edge on the inner land in turn raises the lowest point of the surface, shifting the main bearing outward and thus reducing contact pressure peaks. Furthermore, a 2-level ball cup socket similarly affects hydrostatic deformation, like changing base socket height. The diameter of this additional socket influences the inflection point of the running surface, and if the socket is conical, it smooths transitions between outer lands, reducing edge pressure. In Fig. 9 it is apparent that the geometry of the throttle bore outlet, particularly its height and diameter, significantly changes the running surface deformation. A long throttle outlet appears to be unfavorable, although this length cannot be freely selected due to the throttle geometry. Another occasionally encountered design feature of the base socket is the use of a groove on its outside. This appears to influence the deformation only slightly and in no clear direction.

A common method to increase the swivel angle is by inverting the slipper ball joint, creating an “inverted” slipper. Figure 10 shows that this design leads to greater running surface deformation, as the piston force is concentrated in the center of the base socket and is not guided through the neck into the running surface. For an inverse slipper entirely made of brass, the deformation is more than three

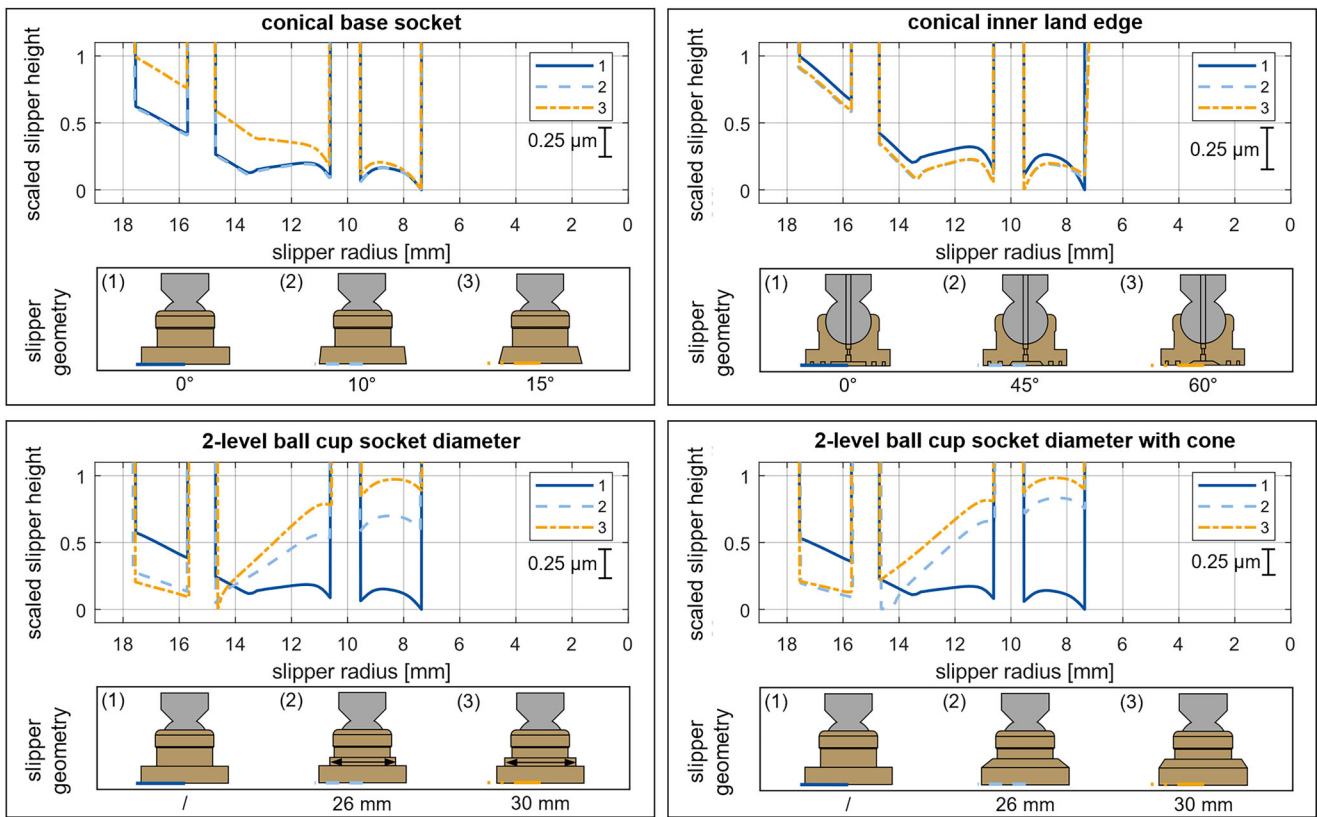


Fig. 8 Geometry study results for 2-level socket and cones

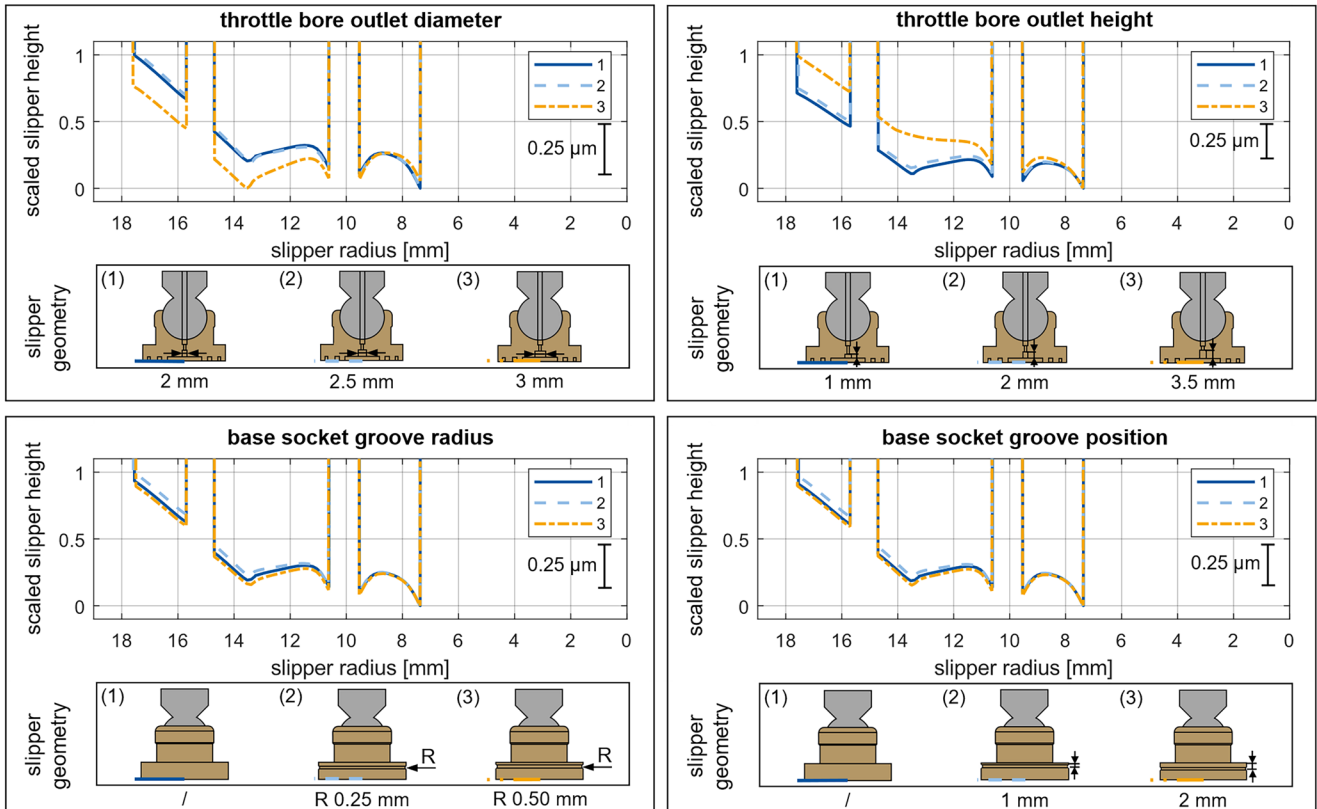
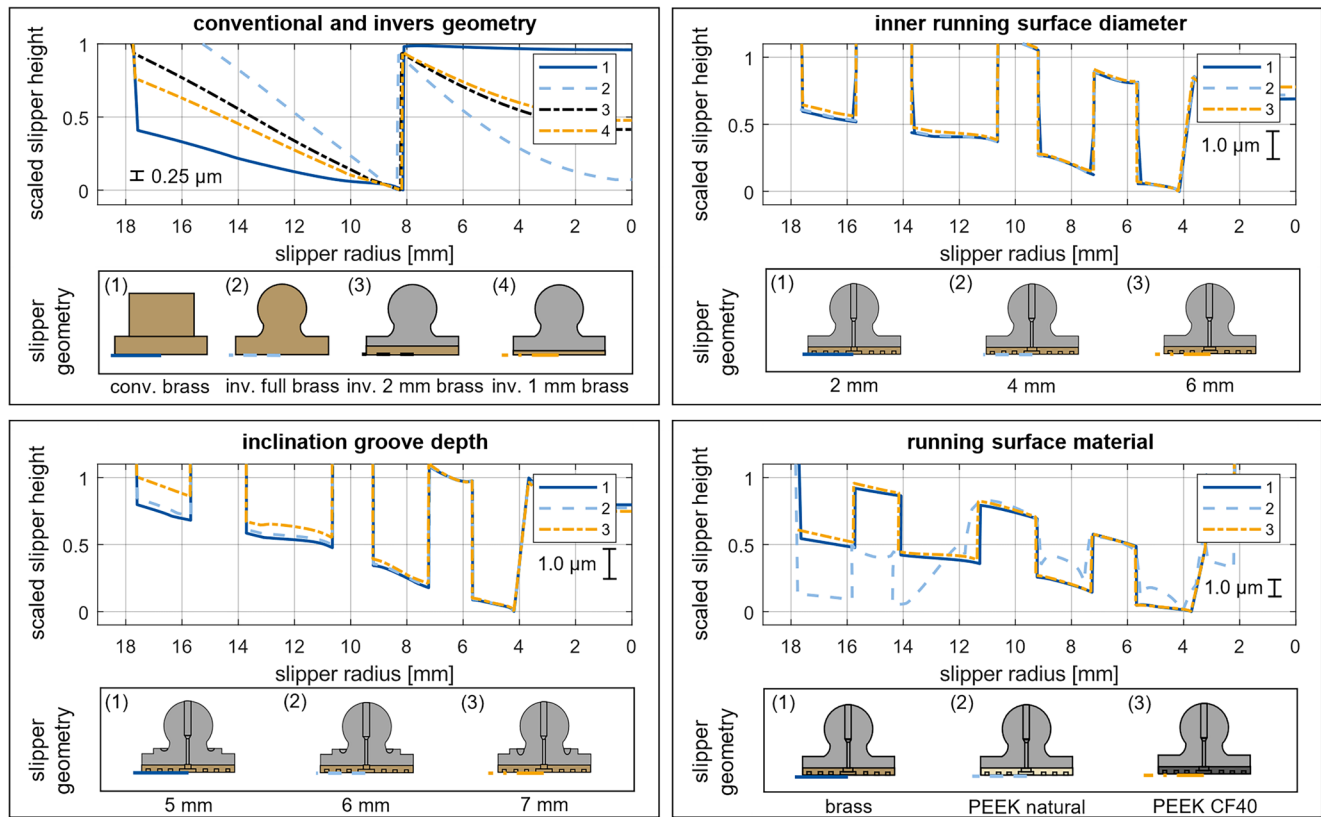


Fig. 9 Geometry study results for the throttle outlet and socket grooves





**Fig. 10** Geometry study results for inverse and plastic slippers

times higher than for the conventional slipper, as can be seen in Fig. 10. The conventional slipper (1) is the same as in the graphics shown above. To reduce this deformation and to increase slipper neck strength, the slipper body can be made of steel with a non-ferrous metal running surface. Deformation decreases with thinner running surfaces, but a larger inner radius increases edge deformation. Another method for increasing the swivel angle even more are inclination grooves, used to enhance slipper tilting. These grooves further increase deformation, leading to the conclusion that methods to increase the swivel angle worsen gap deformation properties. Despite this, the study explores inverse plastic slippers below, as only inverse steel versions are currently available, which could potentially be adapted with plastic running surfaces in future research. Figure 10 shows that using CFR materials like PEEK-CF40 achieves similar deformation to brass. Non-ferrous metal running surfaces are typically joined to steel bases by soldering or friction welding. For plastic slippers, alternative fastening methods must be developed to handle frictional forces.

Figure 11 compares various force-fit and form-fit fastening methods, showing that form-fit variants with surface overlap are particularly effective concerning surface deformation.

A conical fastening leads to greater deformations than a form-fit fixation. In Fig. 11 (bottom right), it is evident

that the increased plastic wall thickness in the slippers center causes a significant lifting of the inner lands. Figure 4 shows that a  $1\text{ }\mu\text{m}$  difference in gap height can result in several MPa difference in contact pressure. As a result, the contact pressure in the lifted areas is significantly decreased. However, since the contact must still support the entire load, this leads to pressure peaks at the lower regions, particularly at the edges near the 4 mm and 14 mm radii. To summarize, the author designed two plastic slippers based on the geometry in Fig. 5, with their deformation shown in Fig. 12. One features thin lands, offering better deformation and suitability for a broader operating range due to reduced hydrodynamics. The other has wider lands, which worsen deformation but lower average contact pressure through increased surface area. Both designs include 2 outer and 3 inner support lands, a multi-stage conical base matching the land arrangement, no inclination grooves or socket grooves, and external form-fit fastening. It should be noted that while the multi-land design favors deformations, previous research indicates higher wear of such a design in heavily solid-contaminated oil [32]. Future experiments must determine which design performs better.

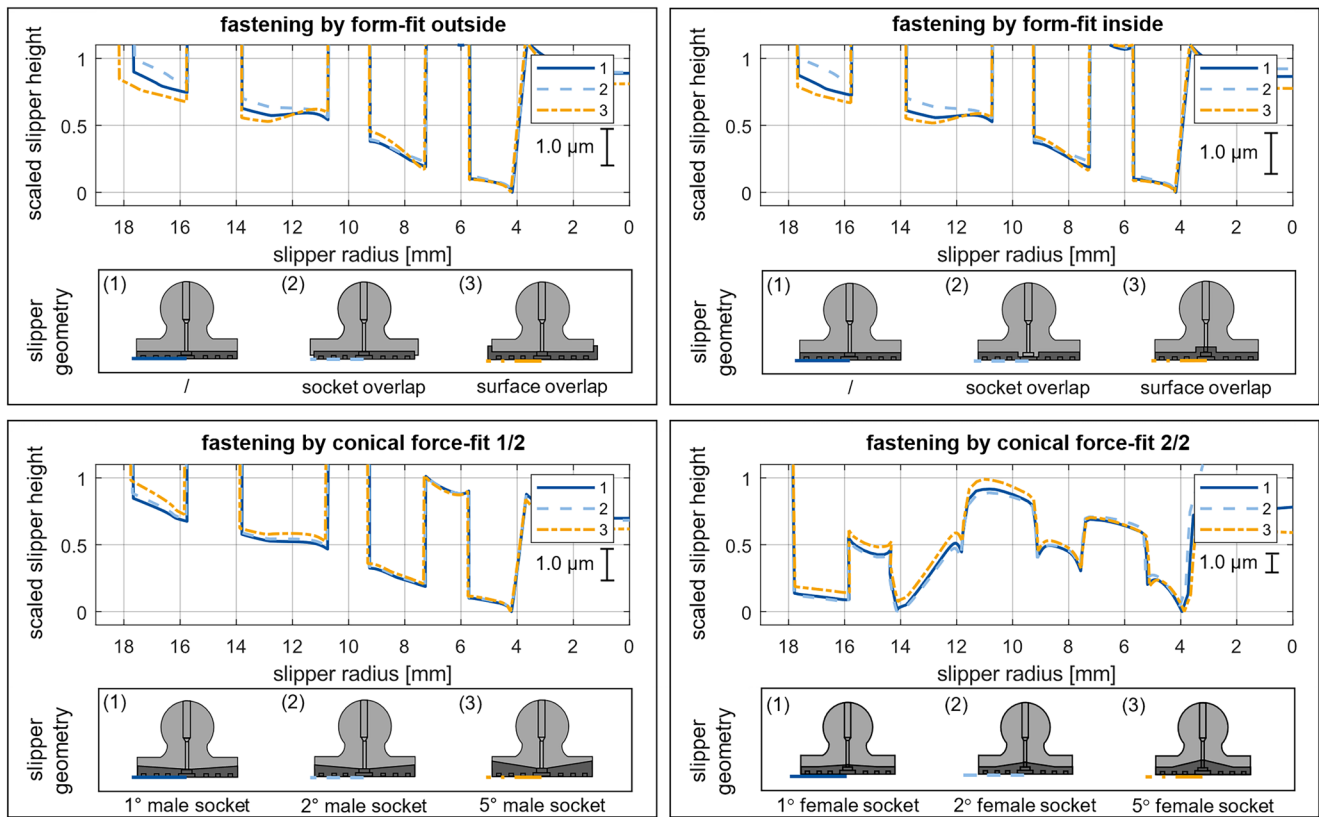


Fig. 11 Geometry study results for the running surface fastening

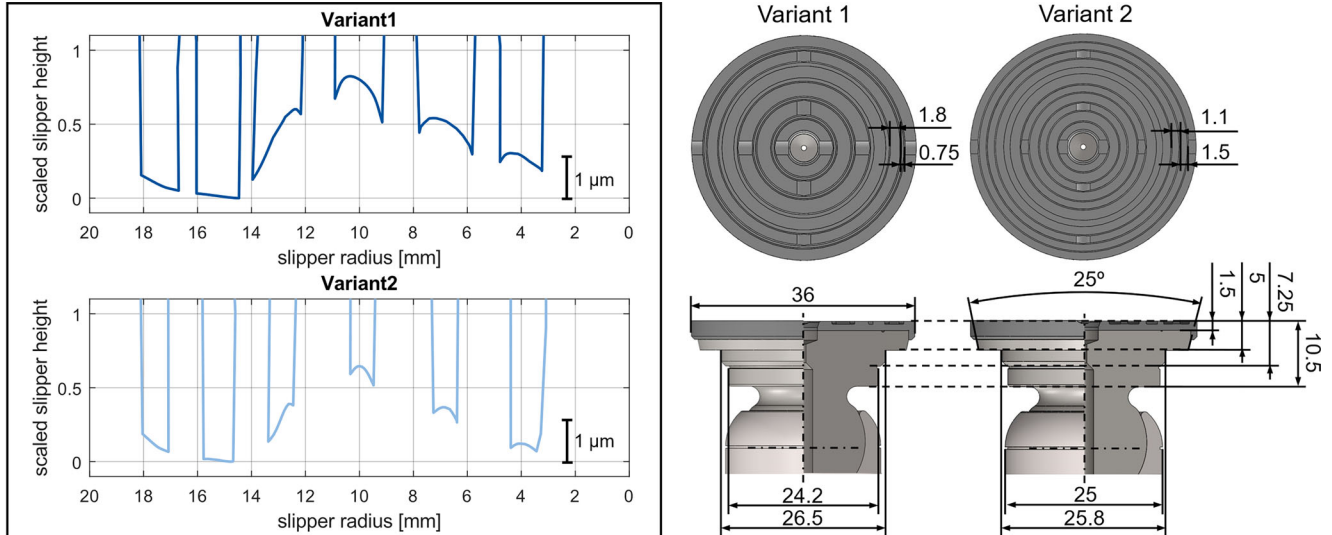


Fig. 12 Geometry of two slippers optimized for plastic running surfaces

## 4 Conclusion and outlook

This paper addresses the need to replace current slipper bearing materials due to issues like toxicity and oil aging. Fiber-reinforced high-performance plastics are proposed as an alternative, though they present design challenges due to increased wear. To use plastics effectively, it is crucial to

reduce the slipper's load, which is primarily possible by enhancing hydrostatic relief. In addition to exact knowledge of all forces acting on the slipper, a calculable, uniform running surface deformation is key for a borderline tuning of hydrostatic relief and preventing excessive wear from localized contact pressure increases. FEM studies have shown that adjusting the ball cup socket diameter and base socket

height can minimize running surface deformation. Multi-stage sockets and cones on the socket and the inner slipper edge can further stabilize deformation. The study also indicates that plastic slippers can achieve similar deformation patterns like brass slippers and that form-fit fastenings for plastic running surfaces are feasible. Future work will involve EHL simulations to assess how hydrostatic pressure changes with deformation impact the results shown here and to precisely calculate all slipper forces. Finally some test slippers will be qualified in a test rig to evaluate the potential of polymer slipper bearings.

**Acknowledgements** This publication was created as part of the research project “validation of a simulation methodology for the design of additively manufactured polymer slippers for oil-hydraulic piston machines” funded by the German Research Foundation DFG (funding code SCHM 3289/18-1). The authors would like to thank the DFG for this support.

**Funding** The research leading to these results received funding from the German Research Foundation (Deutsche Forschungsgemeinschaft) DFG with the project title “validation of a simulation methodology for the design of additively manufactured polymer slippers for oil hydraulic piston machines” with the founding project number 531424256.

**Author Contribution** All authors contributed to the study conception and design. Material preparation, data collection and analysis were performed by Felix Schlegel. The first draft of the manuscript was written by Felix Schlegel and Katharina Schmitz commented on previous versions of the manuscript. All authors read and approved the final manuscript.

**Funding** Open Access funding enabled and organized by Projekt DEAL.

## Declarations

**Conflict of interest** F. Schlegel and K. Schmitz declare that they have no competing interests.

**Ethical standards** For this article no studies with human participants or animals were performed by any of the authors. All studies mentioned were in accordance with the ethical standards indicated in each case.

**Open Access** Dieser Artikel wird unter der Creative Commons Namensnennung 4.0 International Lizenz veröffentlicht, welche die Nutzung, Vervielfältigung, Bearbeitung, Verbreitung und Wiedergabe in jeglichem Medium und Format erlaubt, sofern Sie den/die ursprünglichen Autor(en) und die Quelle ordnungsgemäß nennen, einen Link zur Creative Commons Lizenz beifügen und angeben, ob Änderungen vorgenommen wurden. Die in diesem Artikel enthaltenen Bilder und sonstiges Drittmaterial unterliegen ebenfalls der genannten Creative Commons Lizenz, sofern sich aus der Abbildungslegende nichts anderes ergibt. Sofern das betreffende Material nicht unter der genannten Creative Commons Lizenz steht und die betreffende Handlung nicht nach gesetzlichen Vorschriften erlaubt ist, ist für die oben aufgeführten Weiterverwendungen des Materials die Einwilligung des jeweiligen Rechteinhabers einzuholen. Weitere Details zur Lizenz entnehmen Sie bitte der Lizenzinformation auf <http://creativecommons.org/licenses/by/4.0/deed.de>.

## References

1. Findeisen D, Helduser S (2015) *Ölhydraulik handbuch der hydraulischen antriebe und steuerungen*, 6th edn. Springer Vieweg, Berlin Heidelberg
2. Manring ND (2013) *Fluid power pumps & motors analysis, design, and control*. McGraw-Hill, New York
3. Ivantysyn J, Ivantysynova M (2001) *Hydrostatic pumps and motors: principles, design, performance, modeling, analysis, control and testing*. Akad. Books Internat, New Delhi
4. Schlegel F, Schmitz K (2024) Design study on oil-hydraulic axial piston machine slippers made of conventional non-ferrous metal and tribologically optimized plastics. Accepted manuscript to be published. In: *International journal of fluid power systems*
5. Haidak G, Wang D, Lisiane EAE (2020) Modelling of deformation and failure of slipper-retainer assembly in axial piston machine. *Eng Fail Anal* 111:104490. <https://doi.org/10.1016/j.engfailanal.2020.104490>
6. Reetz B, Münch T (2020) Challenges for novel lead-free Alloys in Hydraulics, 12th International Fluid Power Conference (12. IFK). 1(1):17–25. <https://doi.org/10.25368/2020.6>
7. Holzer A, Reetz B, Münch T, Schmitz K (2022) Experimentelle untersuchung zum einlaufverhalten bleifreier sondermessinglegierungen. *Tribol Schmierungstechnik* 69(1):16–32. <https://doi.org/10.24053/TuS-2022-0003>
8. Ivantysyn R, Horn S, Weber J (2022) Design of a lead-free slipper bearing for low speed axial piston pump applications. 2022 IEEE Global Fluid Power Society PhD Symposium, Neapel Italy
9. Wu H, Zhao L, Ni S et al (2020) Study on friction performance and mechanism of slipper pair under different paired materials in high-pressure axial piston pump. *Friction* 8:957–969. <https://doi.org/10.1007/s40544-019-0314-2>
10. Kalin M, Majadić F, Vižintin J et al (2008) Analyses of the long-term performance and tribological behavior of an axial piston pump using diamondlike-carbon-coated piston shoes and biodegradable oil. *ASMEJ Tribol* 130(1):11013. <https://doi.org/10.1115/1.2805442>
11. Schuhler G, Jourani A, Bouvier S et al (2018) Efficacy of coatings and thermochemical treatments to improve wear resistance of axial piston pumps. *Tribol Int* 126:376–385. <https://doi.org/10.1016/j.triboint.2018.05.007>
12. Rizzo G, Massarotti GP, Bonanno A et al (2015) Axial piston pumps slippers with nanocoated surfaces to reduce friction. *Int J Fluid Power* 16(1):1–10. <https://doi.org/10.1080/14399776.2015.1006979>
13. Tang H, Ren Y, Zhang X (2020) Tribological performance of MoS<sub>2</sub> coating on slipper pair in axial piston pump. *Jcentsouth Univ* 27:115–1529. <https://doi.org/10.1007/s11771-020-4387-x>
14. Holzer A, Koss S, Rosefort J et al (2023) EHLA-coated carbide-reinforced control plates in axial piston pumps first results from real-life application. In: Stryczek J, Warzyńska U (eds) *Advances in hydraulic and pneumatic drives and control*. NSHP 2023. Lecture Notes in Mechanical Engineering. Springer, Cham [https://doi.org/10.1007/978-3-031-43002-2\\_22](https://doi.org/10.1007/978-3-031-43002-2_22)
15. Stryczek J, Banaś M, Krawczyk J (2017) The fluid power elements and systems made of plastics. *Procedia Eng* 176:600–609. <https://doi.org/10.1016/j.proeng.2017.02.303>
16. Danfoss A/S High Pressure Pumps (2023). Service guide—APP pumps—APP 21–46 and APP WHC 15–30 Disassembling and assembling. [Hpp.danfoss.com](http://danfoss.com), dok.no.: AX274339308034en-000302
17. Yang Y, Yankey RP, Li H (2022) Research on the friction pairs in water hydraulic piston pumps. *J Phys Conf Ser* 2218:12067. <https://doi.org/10.1088/1742-6596/2218/1/012067>

18. Liu Y, Wu D, He X et al (2009) Materials screening of matching pairs in a water hydraulic piston pump. *Ind Lubr Tribol* 61(3):173–178. <https://doi.org/10.1108/00368790910953695>
19. Archard JF (1961) Single contacts and multiple encounters. *J Appl Phys* 32:1420–1425. <https://doi.org/10.1063/1.1728372>
20. Ma K, Wu D, Xu R et al (2022) Experimental investigation and theoretical evaluation on the leakage mechanisms of seawater hydraulic axial piston pump under sea depth circumstance. *Eng Fail Anal* 142:106848. <https://doi.org/10.1016/j.engfailanal.2022.106848>
21. Li D, Ma X, Wang S et al (2023) The difference in tribological characteristics between CFRPEEK and stainless steel under water lubrication in friction testing machine and axial piston pump. *Lubricants* 2023(11):158. <https://doi.org/10.3390/lubricants11040158>
22. Guan Z, Wu D, Cheng Q (2020) Friction and Wear characteristics of CF/PEEK against 431 stainless steel under high hydrostatic pressure water lubrication. *Mater Des* 196:109057. <https://doi.org/10.1016/j.matdes.2020.109057>
23. Li D, Ma X, Wang S et al (2024) Failure analysis on the loose closure of the slipper ball-socket pair in a water hydraulic axial piston pump. *Eng Fail Anal* 155:107718. <https://doi.org/10.1016/j.engfailanal.2023.107718>
24. Li D, Li G, Han J (2020) Thermodynamic characteristics research of a water lubricating axial piston pump. *Proc Inst Mech Eng Part C: J Mech Eng Sci* 234(19):3873–3889. <https://doi.org/10.1177/0954406220916538>
25. Nie SL, Huang GH, Li YP (2006) Tribological study on hydrostatic slipper bearing with annular orifice damper for water hydraulic axial piston motor. *Tribol Int* 39(11):1342–1354. <https://doi.org/10.1016/j.triboint.2005.10.007>
26. Rokala M (2012) Analysis of slipper structures in water hydraulic axial piston pumps. Dissertation. Tampere University of Technology
27. Rokala M, Caloni O, Koskinen KT et al (2008) Study of lubrication conditions in slipper-swashplate contact in water hydraulic axial piston pump test rig. *Proc Jfps Int Symp Fluid Power* 2008(7-1):91–94. <https://doi.org/10.5739/isfp.2008.91>
28. Schoemacker F, Murrenhoff H (2018) Piston slippers for robust water hydraulic pumps. In: *Fluid power networks: proceedings: 19th–21th march 2018: 11th international fluid power conference*, [Bd, vol 1, pp 237–247 <https://doi.org/10.18154/RWTH-2018-224355>
29. Schlegel F, Hofmeister M, Osmanovic D et al (2024) Swelling, wear and property changes of high-performance polymers in oil-hydraulic tribological contacts. Accepted Manuscript to be published. In: *Tribologie und Schmierungstechnik*
30. Greenwood JA, Tripp JH (1970) The contact of two nominally flat rough surfaces. *Proc Inst Mech Eng* 185(1):625–633. [https://doi.org/10.1243/PIME\\_PROC\\_1970\\_185\\_069\\_02](https://doi.org/10.1243/PIME_PROC_1970_185_069_02)
31. McCool JJ (1987) Relating profile instrument measurements to the functional performance of rough surfaces. *Asme J Tribol* 109(2):264–270. <https://doi.org/10.1115/1.3261349>
32. Jacobs G (1993) Verschleißverhalten hydraulischer pumpen und ventile beim betrieb mit feststoffverschmutztem Öl, dissertation. RWTH Aachen

**Publisher's Note** Springer Nature remains neutral with regard to jurisdictional claims in published maps and institutional affiliations.